

Magnetic Nulls in Kinetic Simulations of Space Plasmas

Vyacheslav Olshevsky^{1,2}

sya@mao.kiev.ua

Jan Deca, Maria Elena Innocenti, Emanuele Cazzola, Ivy Bo Peng,
Andrey Divin, Elin Eriksson, Stefano Markidis, Giovanni Lapenta

Center for mathematical Plasma Astrophysics, KU Leuven, Belgium

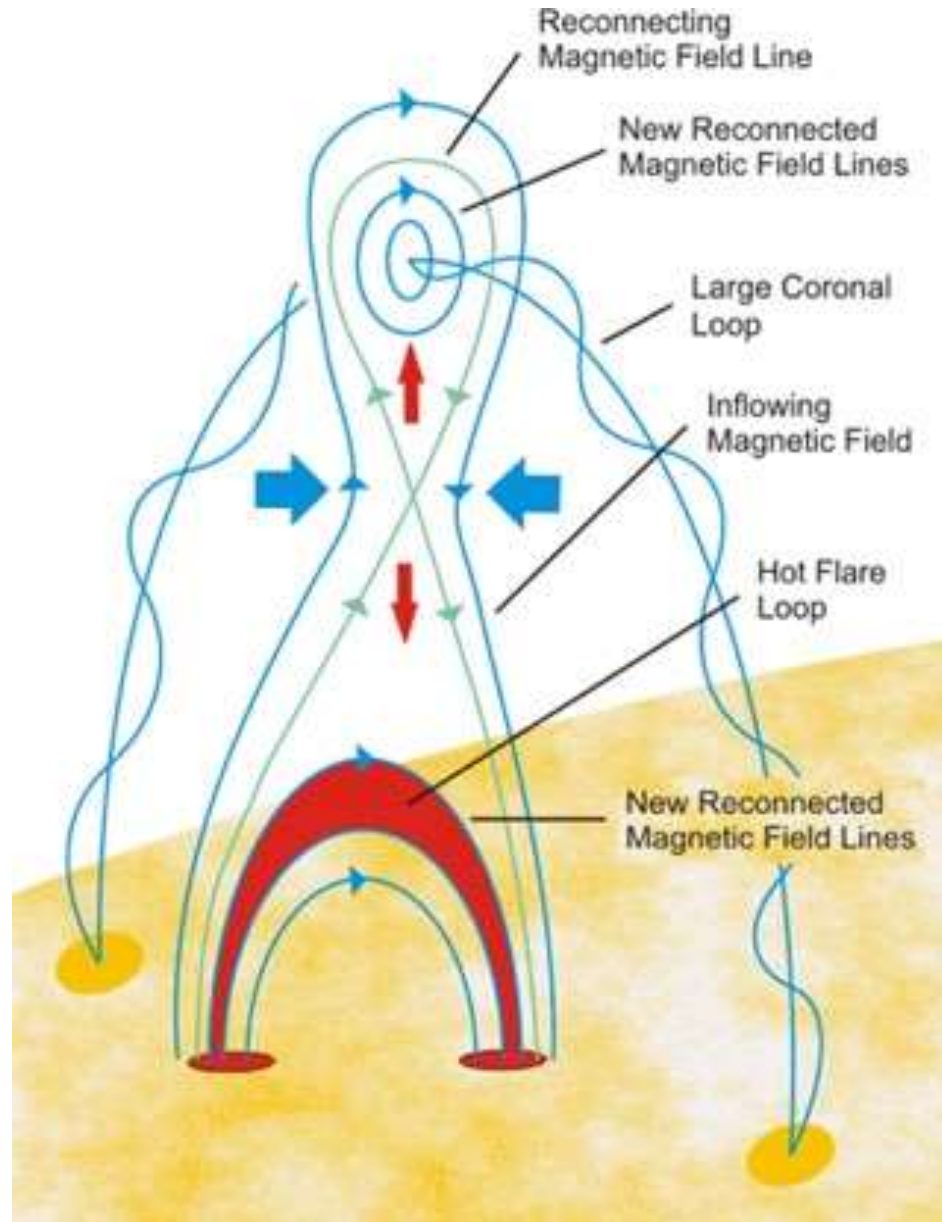
Main Astronomical Observatory, Kyiv, Ukraine

KTH Royal Institute of Technology, Stockholm, Sweden

Swedish Institute of Space Physics, Uppsala, Sweden

St. Petersburg State University, Russia

Magnetic nulls in solar flares



Magnetic nulls in PFSS models

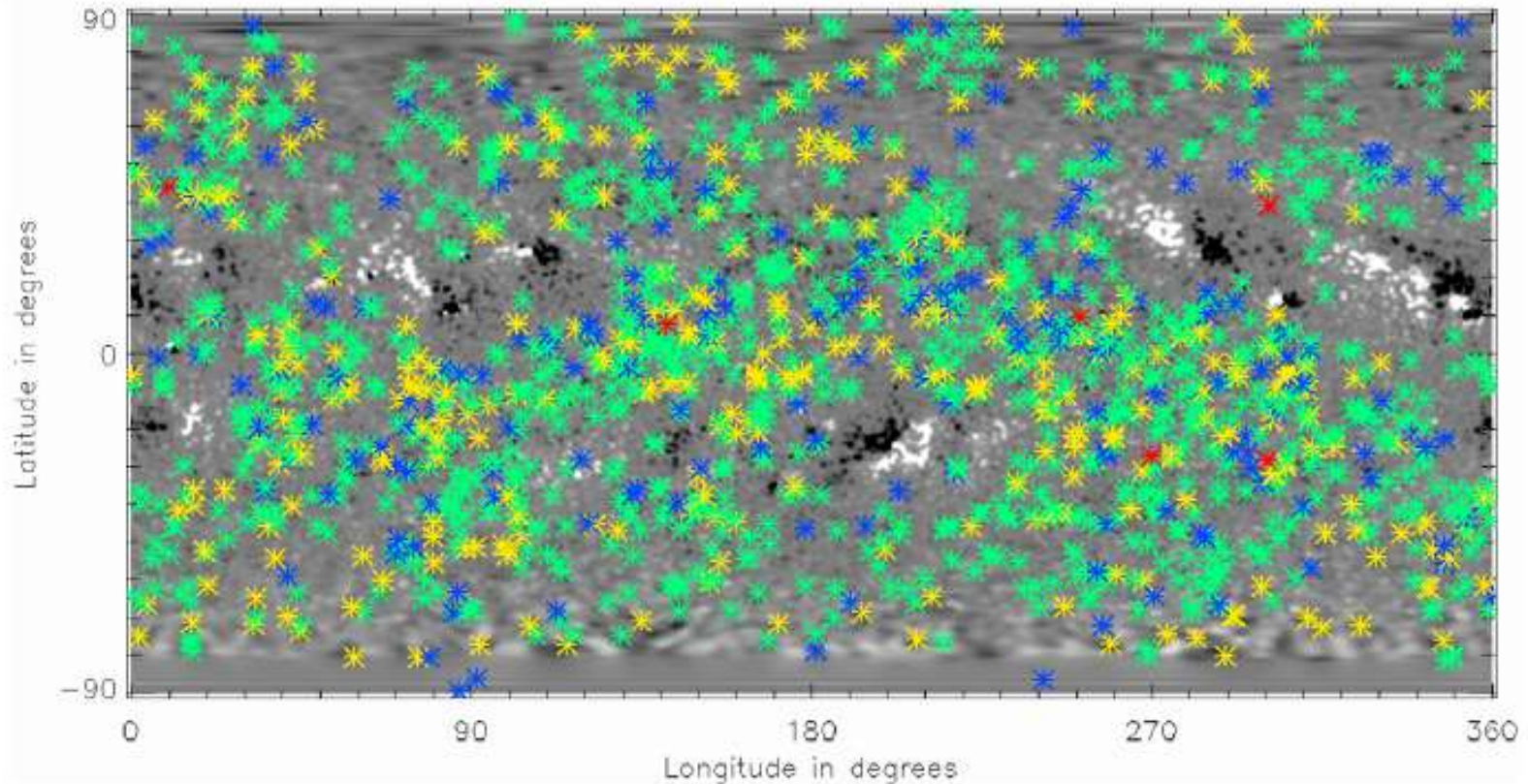


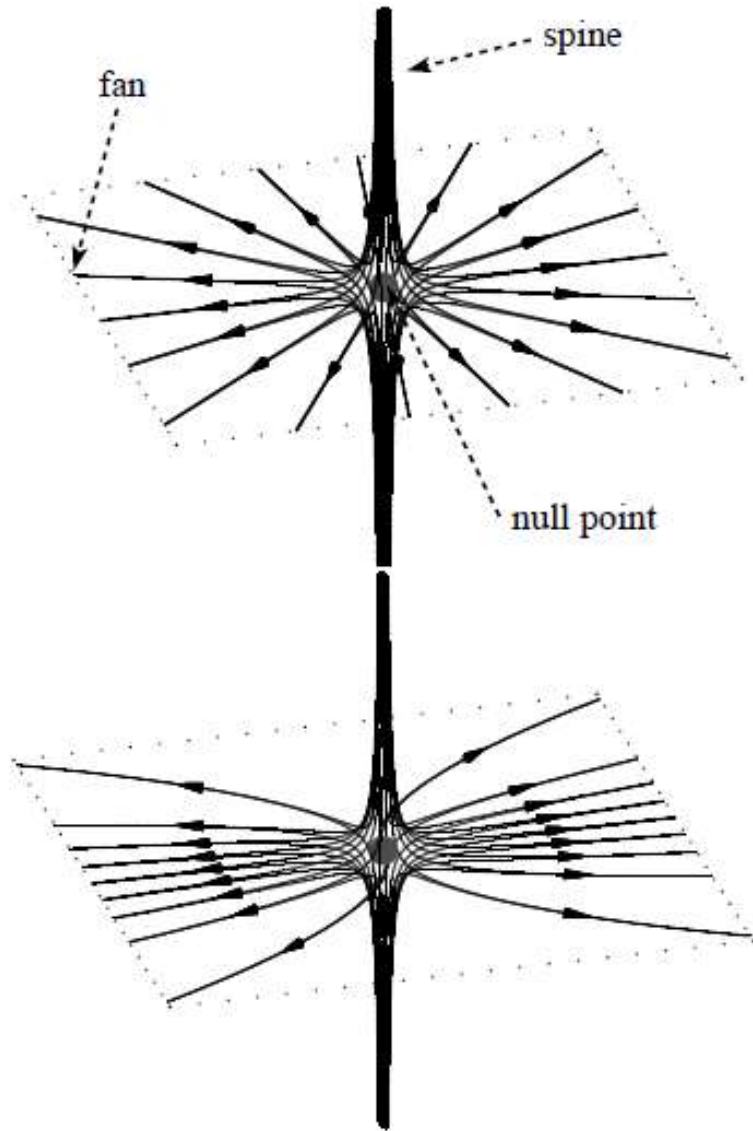
Figure 7 Positions of null points in the PFSS extrapolations for Carrington rotation 2100 44 from (a) HMI, (b) MDI, and (c) SOLIS over-plotted on the corresponding radial component of the magnetic field at the photosphere. Blue stars are nulls below 0.696 Mm, green stars are nulls between 0.696 Mm and 6.96 Mm, yellow stars are nulls between 6.96 Mm and 69.6 Mm, and red stars are nulls above 69.6 Mm.

Recent interest to nulls

- Fu et al. “How to find magnetic nulls and reconstruct field topology with MMS data?”, JGR 2015
- Eriksson et al. “Statistics and accuracy of magnetic null identification in multispacecraft data”, GRL 2015
- Edwards & Parnell “Null Point Distribution in Global Coronal Potential Field Extrapolations”, SoPh 2015
- Wyper & Pontin “Non-linear tearing of 3D null point current sheets”, 2014 PhPI
- Wendel & Adrian “Current structure and nonideal behavior at magnetic null points in the turbulent magnetosheath”, 2013 JGR

Our aim: look for nulls in different kinetic simulations.

Null-point classification



$$\mathbf{B}(\mathbf{r}) = \frac{\partial \mathbf{B}}{\partial \mathbf{r}} \cdot \mathbf{r}$$

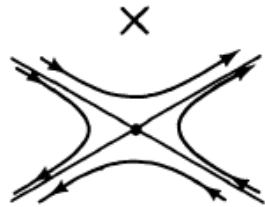
$$\frac{\partial \mathbf{B}}{\partial \mathbf{r}} = \begin{pmatrix} b_{11} & b_{12} & b_{13} \\ b_{21} & b_{22} & b_{23} \\ b_{31} & b_{32} & b_{33} \end{pmatrix}$$

$$\nabla \mathbf{B} = 0 \rightarrow \text{tr} \left(\frac{\partial \mathbf{B}}{\partial \mathbf{r}} \right) = 0$$

3 eigenvalues:

$$\lambda + \mu + \nu = 0$$

Radial and spiral null points



(a)



(b)

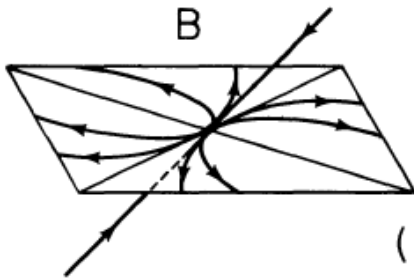
Nulls classification by
Lau & Finn (1990)

Radial nulls

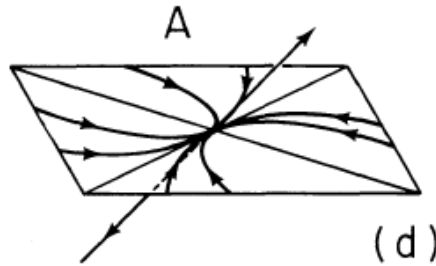
A (negative), B (positive) \rightarrow X

Spiral nulls

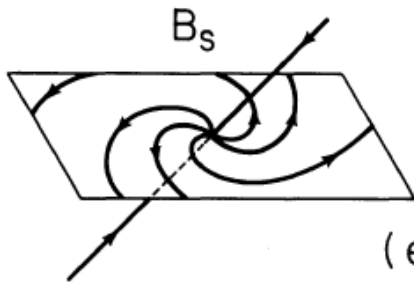
A_s (negative), B_s (positive) \rightarrow O



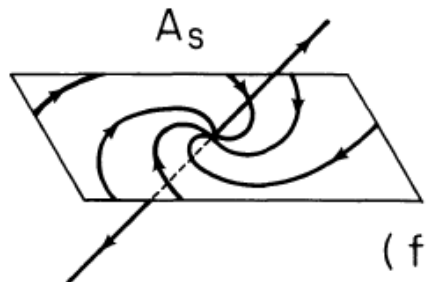
(c)



(d)



(e)



(f)

Locating nulls in simulations

Hairy ball (Poincare-Hopf) theorem: there is no non-vanishing continuous tangent vector field on even-dimensional n -spheres. Topological degree == number of nulls in cell (Greene, 1992).

...**whenever** one attempts to comb a hairy ball flat, there will always be at least one tuft of hair at one point on the ball. (© Wikipedia)



Configurations under study

- Harris current sheet in 3D
- 'Asymmetric reconnection'
- Lunar Magnetic Anomalies
- Planetary mini-magnetospheres
- **"Multiple nulls"** (Olshevsky et al., *Phys Rev. Lett.* 111, 2013)

$$B_x = -B_0 \cos \frac{2\pi x}{L_x} \sin \frac{2\pi y}{L_y},$$

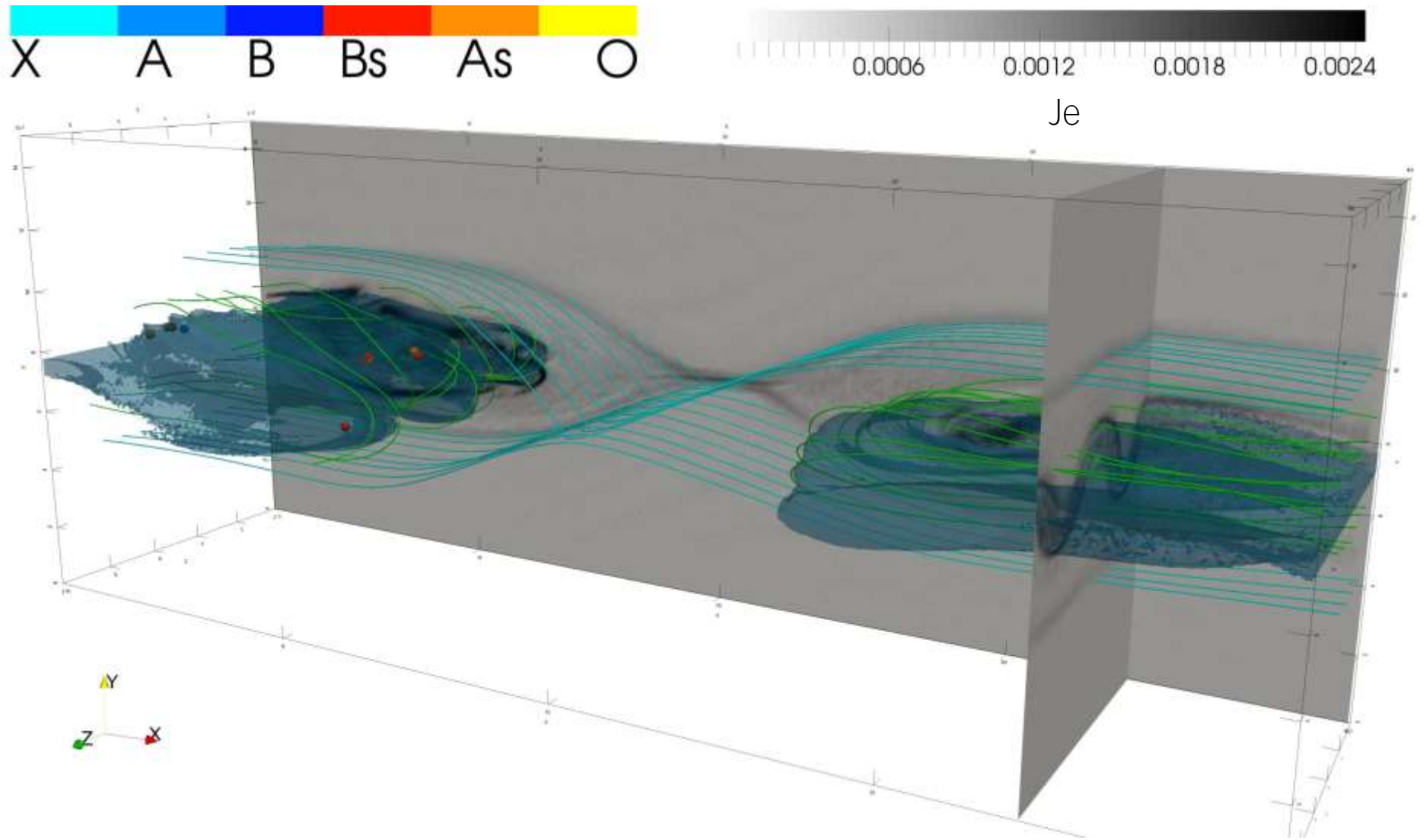
$$B_y = B_0 \cos \frac{2\pi y}{L_y} \left(\sin \frac{2\pi x}{L_x} - 2 \sin \frac{2\pi z}{L_z} \right),$$

$$B_z = 2B_0 \sin \frac{2\pi y}{L_y} \cos \frac{2\pi z}{L_z}.$$

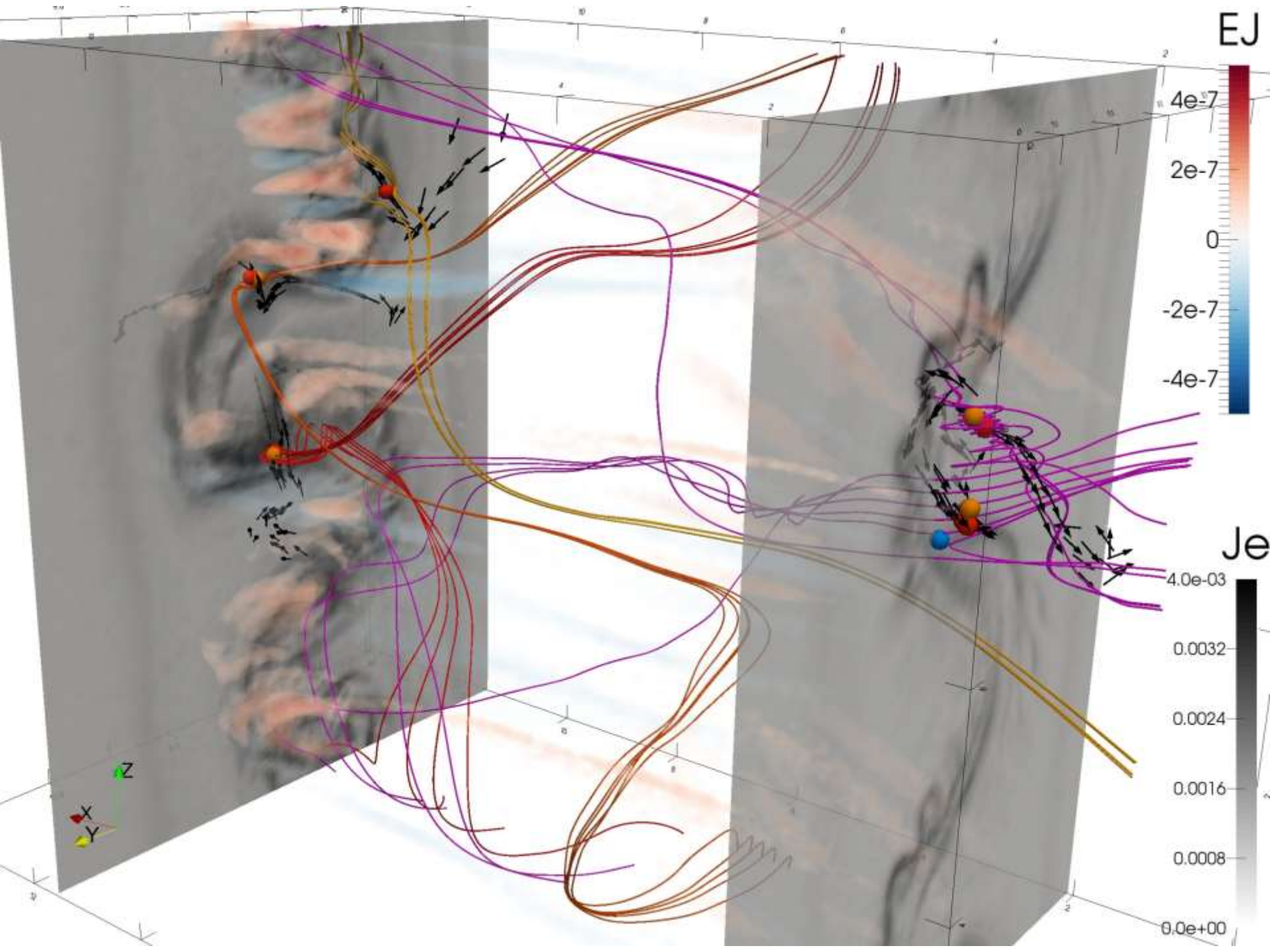
We use topological degree to locate and classify nulls in our simulations.

All simulations done by kinetic Particle-in-Cell code iPic3D (Markidis et al., 2010)

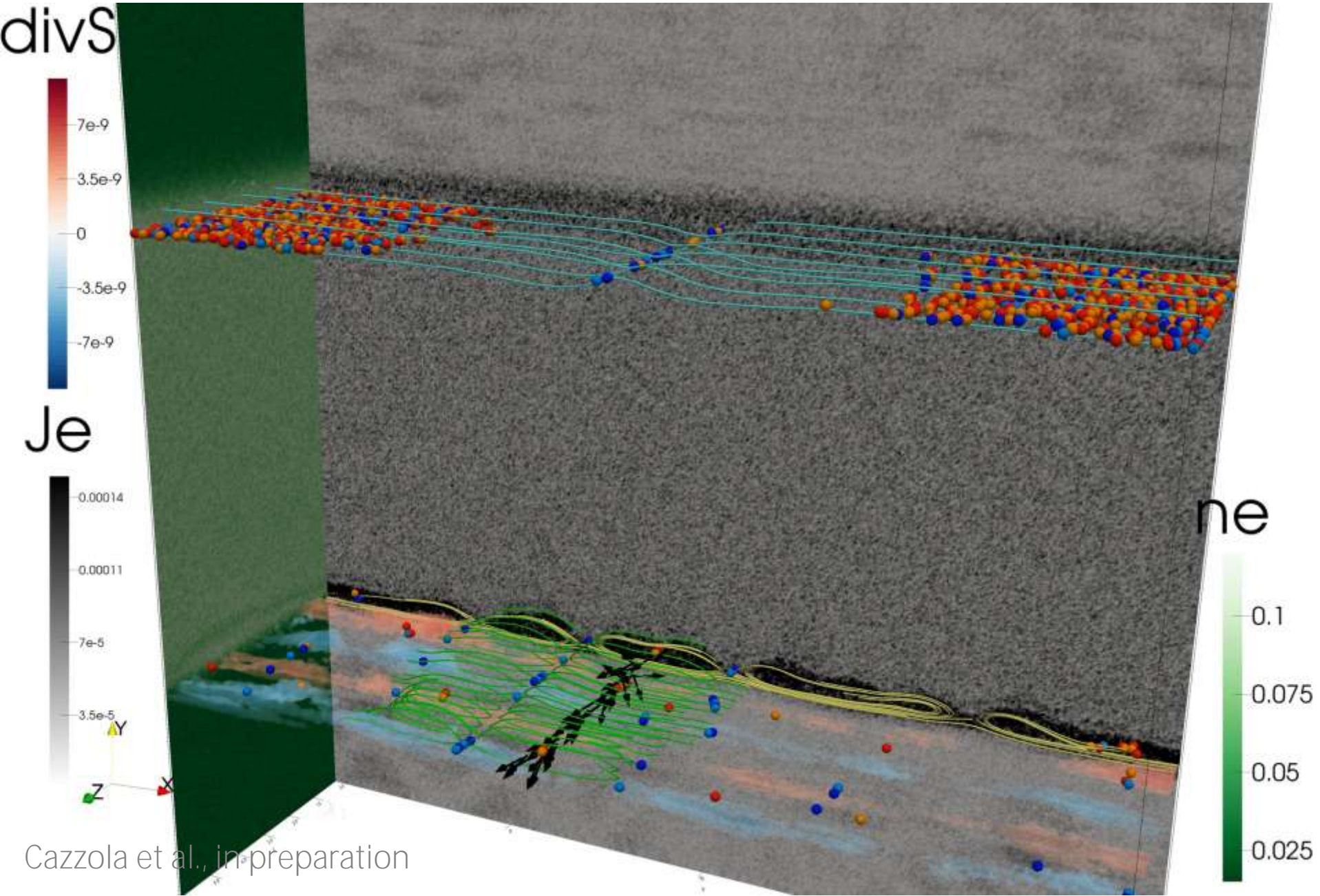
3D Harris sheet with small guide field

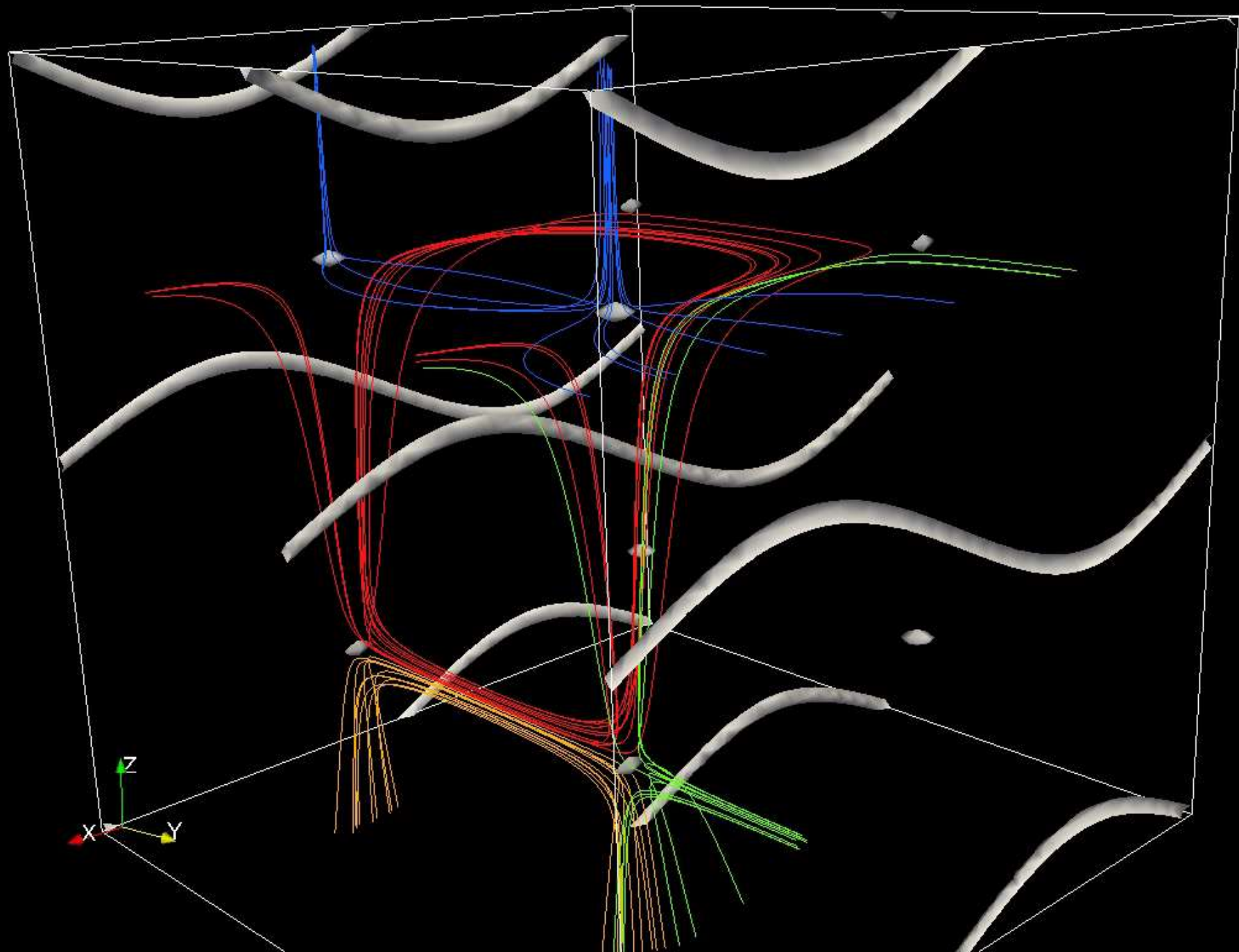


Kinetic PIC simulations by Giovanni Lapenta, Harris current sheet with $B_g=0.1$.

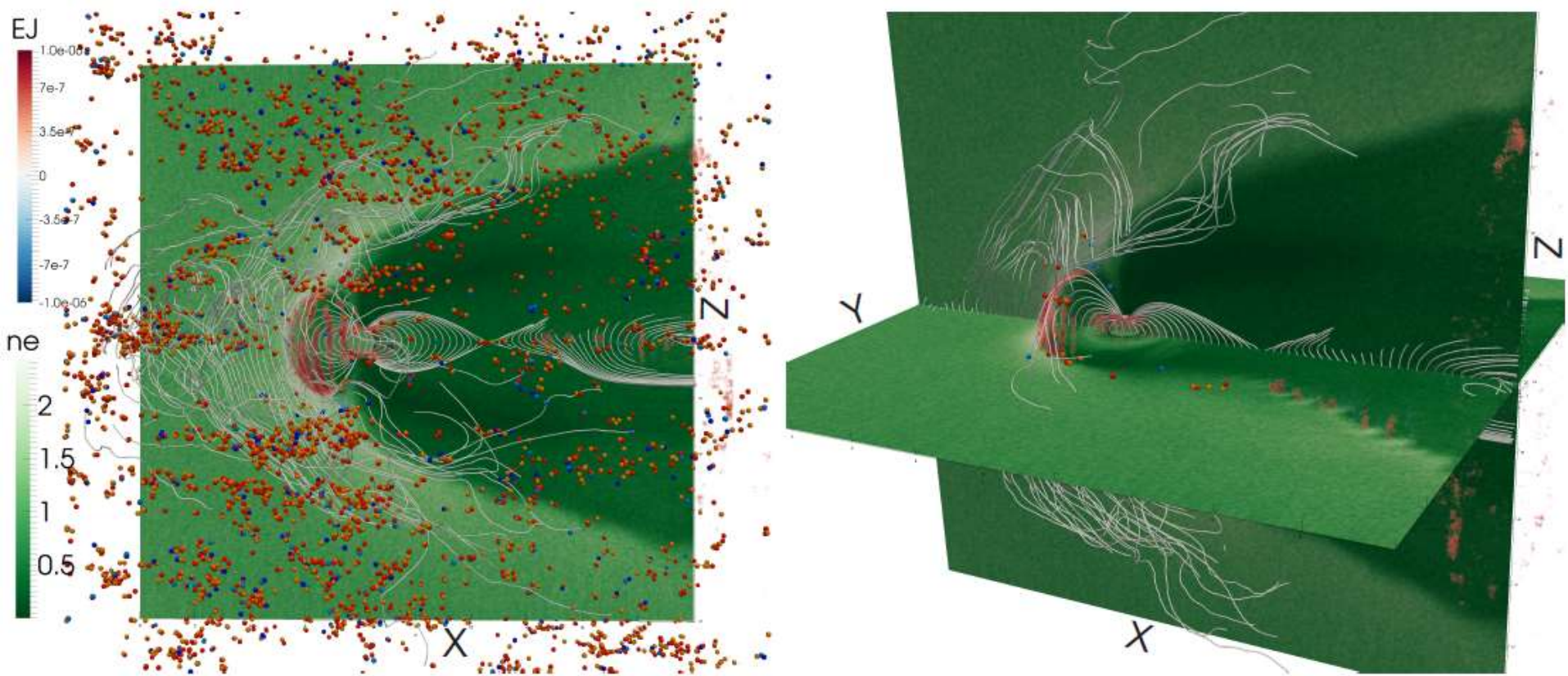


Asymmetric reconnection





Planetary mini-magnetospheres

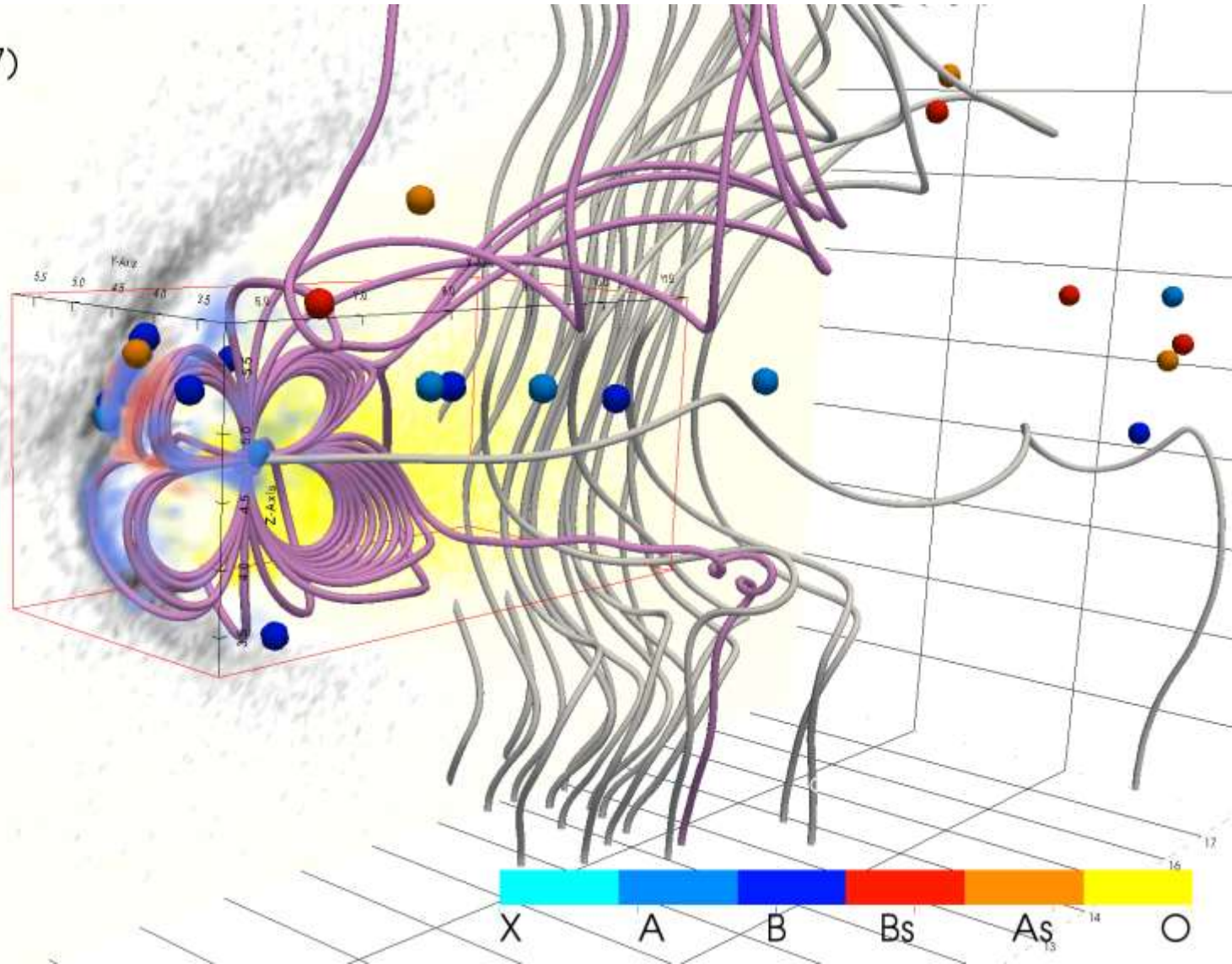
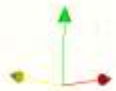
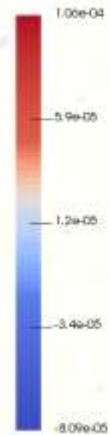


Quadrupolar mini-magnetosphere

density (plane $y=5.7$)

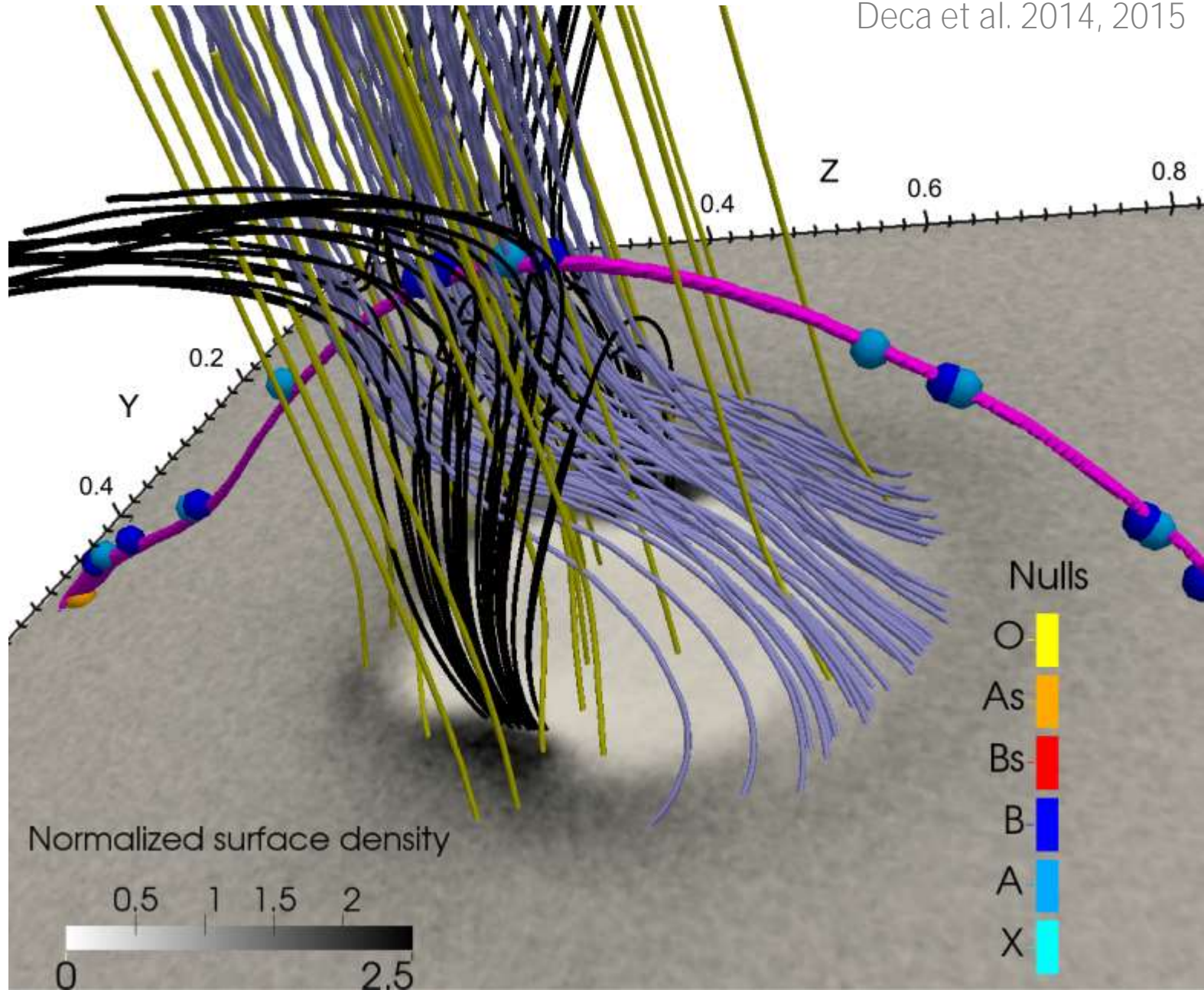


$E \cdot J$



Lunar Magnetic Anomaly

Deca et al. 2014, 2015



Spiral vs Radial nulls

Observations: 80% spiral

Eriksson+ GRL (2015)

	Nulls found	A (%)	B (%)	A_s (%)	B_s (%)
Poincaré index	64	8	1	55	36
Taylor expansion	443	14	8	42	36

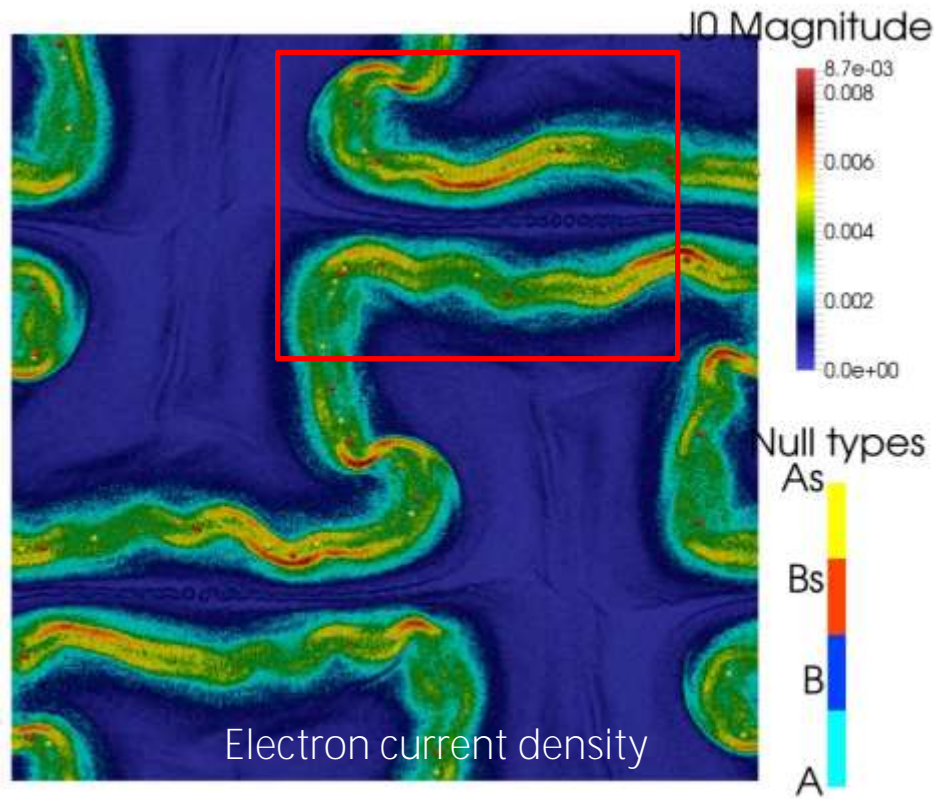
Simulations

Olshevsky et al., submitted to ApJ

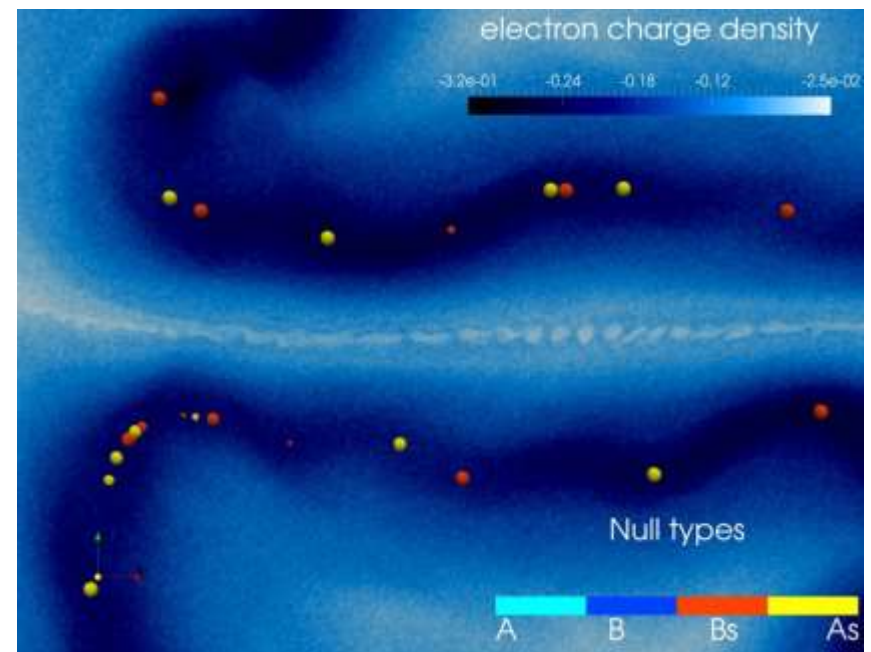
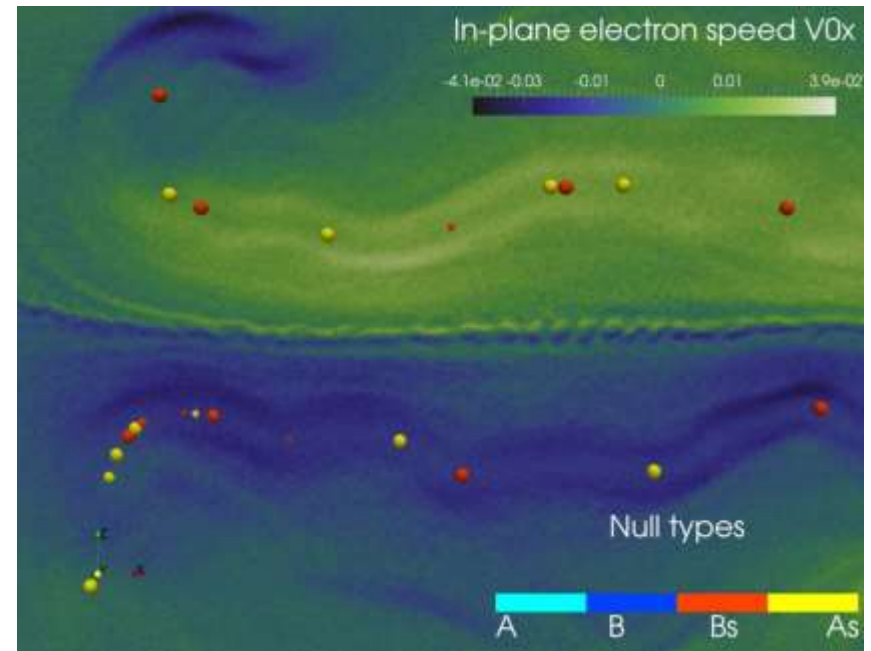
Run	A	B	A_s	B_s	$A_s + B_s$ (%)	Energy dissipation?
Harris $B_g = 0$	3	10	33	32	83	Flux ropes and current filaments.
Harris $B_g = 0.1$	1	0	5	6	92	Flux ropes and current filaments.
Asymmetric	136	141	439	428	76	Flux ropes and current filaments.
Multiple nulls	5	5	54	58	92	Flux ropes (Z-pinches).
Dipole	584	577	3836	3778	87	Bow shock, magnetopause, magnetotail.
Quadrupole	9	9	9	12	54	Bow shock, magnetopause.
LMA	10	11	2	0	9	No reconnection; radial null line.

Spiral nulls inside *magnetic flux ropes* are perhaps more important for energy dissipation than radial nulls.

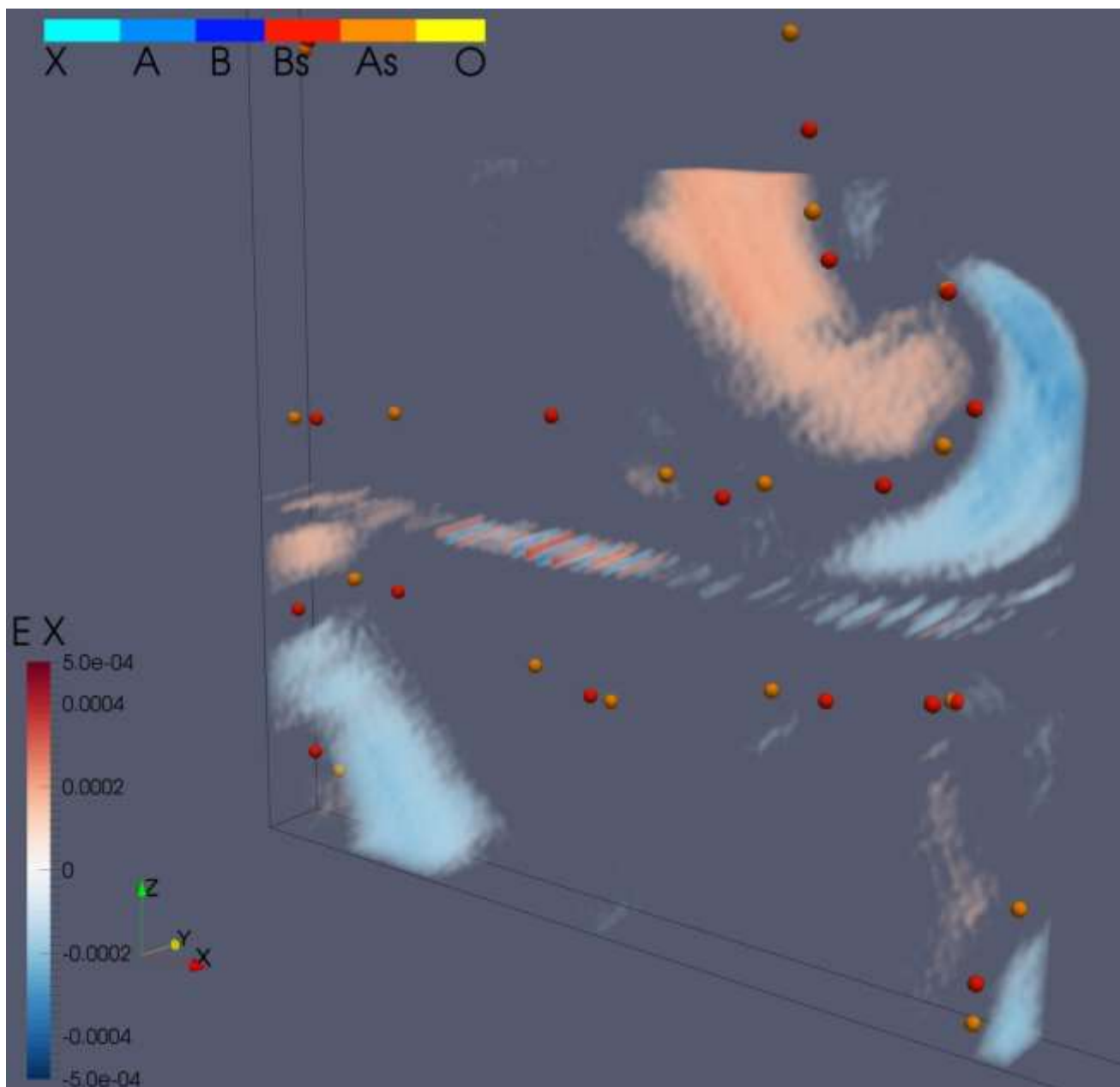
Instability on the interface of two null lines



High-resolution ($0.025 d_j$) simulations reveal small-scale instabilities on the interface of two magnetic flux ropes.

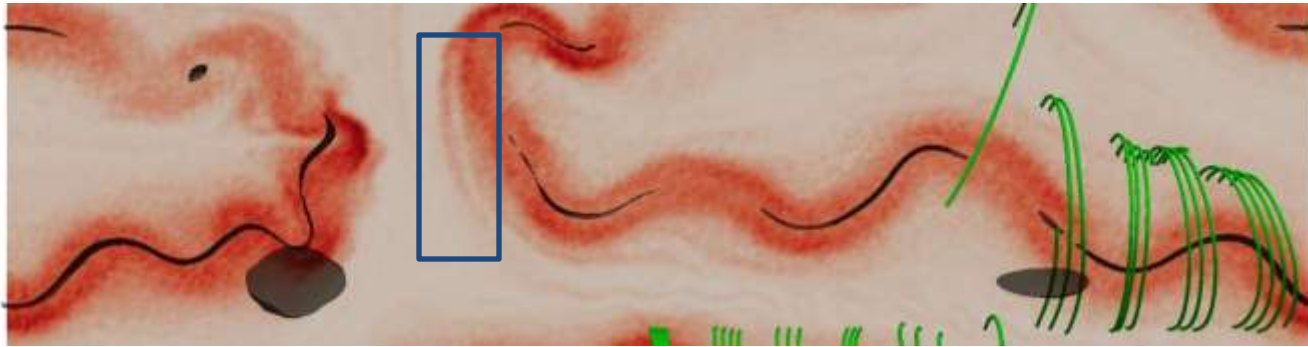


Electron holes on the interface of two streams

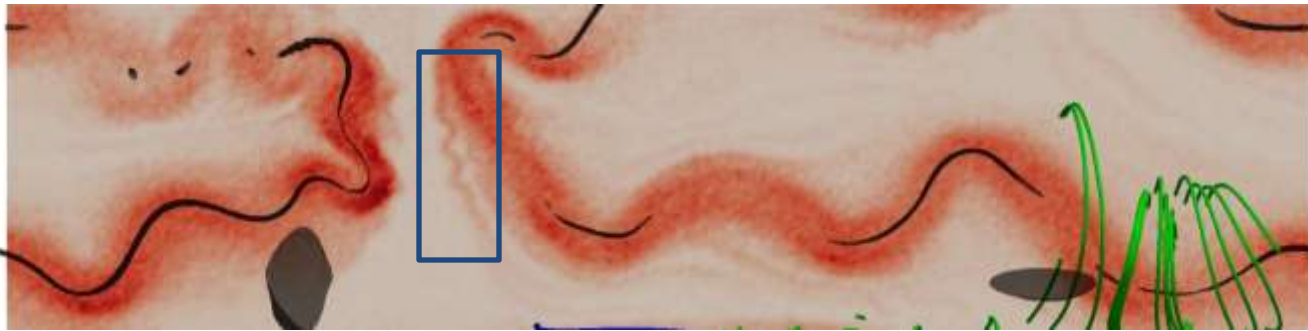


Electron current filamentation

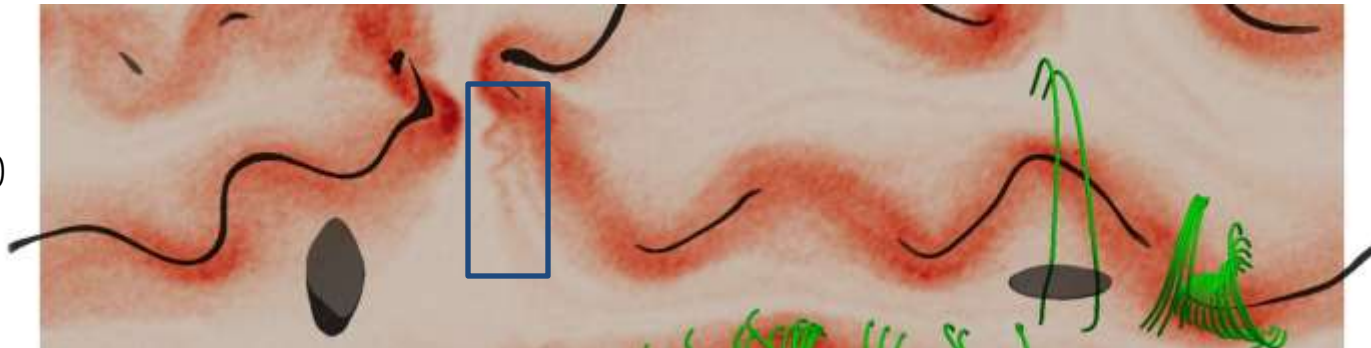
$\omega_{ci}t = 33.8$



$\omega_{ci}t = 36.4$



$\omega_{ci}t = 39.0$



Conclusions & Questions

1. Neither solely concentrate on topology, nor despise it (Lapenta on Monday)
2. Null points are ubiquitous in space plasmas, but often do not indicate magnetic reconnection!
3. Spiral nulls + magnetic flux ropes are dissipating energy (Buechner+ on Tuesday)
4. Energy dissipation mechanisms (energetic events?):
 - kinking
 - two-stream instabilities
 - filamentation/LHDI?